



金属构件激光增材制造缺陷产生机理及控制机制探究

姚讯杰¹, 王佳玮¹, 杨雁程¹, 张馨月¹, 程序^{2*}, 张述泉³

¹北京航空航天大学材料科学与工程学院, 北京 100191;

²北京航空航天大学前沿科学技术创新研究院, 北京 100191;

³北京煜鼎增材制造研究院有限公司, 北京 100096

摘要 高性能金属构件的激光增材制造可以实现复杂零件的“近净成形”, 是近年来航空、航天、船舶海洋等现代重大装备制造业的研究热点。由于增材制造过程中材料的熔凝行为受原材料组分和制备工艺的影响, 一旦材料或成型工艺选择不合理, 成型件会不可避免地出现缺陷, 影响构件性能。因此, 对金属构件激光增材制造中的缺陷产生机理及控制机制进行研究很有必要。总结了近年来金属构件激光增材制造缺陷的控制方法, 归纳了缺陷的种类, 对制造过程中的三种典型缺陷——裂纹、孔隙和夹杂的产生机制进行了分析, 并根据其产生机理针对性地提出了相应的控制机制, 展望了金属构件激光增材制造缺陷控制方法的未来发展方向。

关键词 激光技术; 材料; 激光增材制造; 金属构件; 缺陷; 控制机制

中图分类号 TG14

文献标志码 A

DOI: 10.3788/CJL202249.1402802

1 引言

随着航空、航天、船舶海洋、电力等现代工业所需的材料向轻量化、高可靠性、长服役寿命等方向快速发展, 构件出现尺寸大型化、结构复杂化、功能综合化的特点^[1-3]。大型整体高性能金属构件的成型制备对制造技术要求严苛, 若采用铸造、锻造和轧制等传统制造技术进行制备, 常需要大型装备, 且对于具有复杂结构的构件, 上述工艺加工难度大、制备周期长、生产成本高, 无法实现复杂构件的高效制备。因此, 大型复杂关键金属构件制造技术是航空、航天、船舶海洋等现代重大装备制造业的核心技术^[4]。应用于高性能金属构件制备的激光熔化沉积增材制造通过周期性激光逐点扫描、逐线搭接、逐层熔化凝固堆积, 可实现复杂零件的“近净成形”及复杂构件的“直接制造”^[5-9]。在激光增材制造过程中, 构件经历高能激光束的周期性、剧烈、非稳态、循环加热和冷却作用, 且激光束在构件中发生短时非平衡循环固态相变, 这些过程十分复杂, 一旦原材料或成型工艺选择不合理, 成型件会不可避免地出现缺陷, 影响其性能^[10-11]。如当原材料粉末含有气体时, 激光增材过程中液体的冷凝速度快于气体的逃逸速度, 形成气孔; 当激光功率选择较小时, 所有粉末未能被完全熔化, 形成未熔合孔和夹杂; 当激光与粉末的作用时间极短时, 熔池及其周边的熔化、凝固和冷却速度较快, 热应力较大, 易萌生裂纹等。因此, 国内外许

多学者对激光增材制造成型工艺中的缺陷产生机制进行了广泛研究^[12-17]。金属构件内部的典型缺陷按照尺度可分为宏观缺陷和微观缺陷^[15], 激光增材制造金属构件中常见的缺陷有裂纹、夹杂和孔隙, 其中孔隙为微观缺陷, 裂纹和夹杂为宏观或微观缺陷。本文围绕国内外学者对金属构件激光增材制造中这三类缺陷的产生机理及控制机制研究进行了综述。

2 激光增材制造常见的缺陷种类及产生机理

2.1 裂纹缺陷的产生机理

激光增材制造过程中快速复杂的热循环通常会使金属构件有较大内应力, 萌生微裂纹, 部分微裂纹在后续制造过程中扩展成宏观裂纹。对于激光增材制造中产生的裂纹缺陷, 根据发生的温度区间, 可以将其分为冷裂纹与热裂纹两类。

一般来说, 增材制造过程中产生的冷裂纹常见于含有马氏体的合金, 例如 M2 高速钢。在激光增材制造结束后, 材料在冷却过程中不断收缩, 高能激光束的周期性循环加热致使材料内部的残余应力不断积累, 进而导致应力集中, 产生冷裂纹^[18-20]。冷裂纹的产生通常具有一定的延时性, 一旦产生就开始扩展, 最后材料发生脆性断裂, 因此冷裂纹的危害常常是灾难性的。产生冷裂纹的三个必要条件^[21-22]是: 1) 水分在激光高能束的作用下分解为氢原子并扩散至缺陷夹杂处(根

收稿日期: 2021-10-18; 修回日期: 2022-01-10; 录用日期: 2022-03-10

基金项目: 广东省基础与应用基础研究重大项目(2020B0301030001)

通信作者: *chengxu@buaa.edu.cn

据氢脆理论,在应力梯度作用下,氢原子在晶格内扩散或跟随位错运动到应力集中区域,由于氢和金属原子之间的交互作用使金属原子间的结合力变弱,当氢原子聚集到一定程度时,材料将产生裂纹且裂纹不断扩展);2)激光增材制造产生纵向和横向的残余热应力(当应力增大到超过临界拘束应力时,裂纹产生);3)马氏体含量高(钢的硬度随材料含碳量的增加而增大,塑性显著降低,裂纹敏感性增大)。Kempen 等^[23]在激光选区熔化制造 M2 高速钢的过程中发现,钢材的高硬度低塑性致使残余应力无法释放,大量冷裂纹产生。

相比于冷裂纹,热裂纹在增材制造过程中更为常见。热裂纹是当构件处于较高温度时,在凝固热应力的作用下产生的裂纹^[16,24],主要分为凝固裂纹及液化裂纹两类^[25-26]。凝固裂纹主要是凝固后期树枝晶间的液膜被热应力拉开而产生的,其大致形貌如图 1 所示^[27]。在合金的凝固过程中,根据枝晶形貌和液相补缩能力的不同,存在四个区域:液相区、悬浮区(准液相区)、糊状区(准固相区)及固相区,通常认为凝固裂纹

是在糊状区形成的。研究者提出许多理论解释凝固裂纹现象,例如强度理论、回流愈合理论以及液膜理论等^[28-30];在凝固过程中的不同时间段,裂纹形成的机制不同^[31-32]。强度理论认为,在熔池凝固后期,固相骨架已经形成并开始收缩,由于收缩受阻,糊状区产生应力和变形,当应力超过合金的强度极限或变形超过此温度下合金的承受极限时,便产生凝固裂纹^[33]。Stangeland 等^[31]研究发现,铝合金因线膨胀系数大(约为钢的 2 倍),在增材制造过程中易产生热应力和热变形,因而极易产生凝固裂纹。回流愈合理论认为,凝固裂纹的产生是由于固相开始接触但并未搭接时,分布在枝晶间的液膜的连续断裂未能被液体及时地回流愈合。Wang 等^[34]在激光增材制造过程中发现,适当地增加枝晶间距、加宽液体回流愈合通道可以减少凝固裂纹的产生。液膜理论指出,在凝固后期固相搭接完成时,枝晶间隙处的液膜会以孤立的形式存在,液相已无法完成回流愈合,此时局部应力会造成液膜开裂,进而形成凝固裂纹。

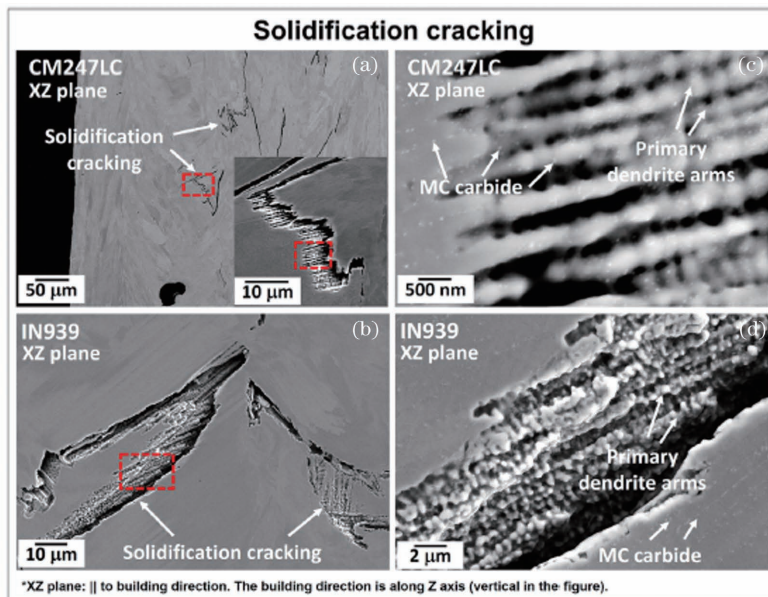


图 1 不同合金中的凝固裂纹^[27]。(a)(c)CM247LC 合金;(b)(d)IN939 合金

Fig. 1 Solidification cracks in different alloys^[27]. (a) (c) CM247LC alloy; (b) (d) In939 alloy

除了凝固裂纹,激光增材制造过程中金属构件易产生的另一种热裂纹就是液化裂纹,如图 2 所示^[27]。液化裂纹是冶金因素和力学因素相互作用的结果,其大致形貌如图 2 所示。液化裂纹产生于脆性温度区间;在该区间内,热影响区的晶界塑性和强度急剧下降,随后冷却过程中产生的拉应变主要集中于液化晶界上,当拉应变超过由液化形成的晶界液膜的塑性变形能力时,金属构件就会沿液化晶界开裂,裂纹沿晶扩展。这类裂纹缺陷在镍基合金中较常见,如 Inconel738 合金和 CM247LC 合金。液化裂纹^[35-36]的形成机制分为两种:一是在激光增材制造高温循环条件下,热影响区偏析形成的低熔点共晶相重熔,并在拉应力作用下开裂;另一种更常见的是在激光增材制造

过程中,在非平衡快速加热作用下,晶界处第二相的熔解和溶质元素的扩散引起了局部晶界液化。Zhong 等^[25]在激光增材制造 Inconel738 合金中发现,枝晶间分布的低熔点 MC 碳化物和 Laves 相在后续的热循环过程中熔化并产生液膜,当凝固开始时,液膜在拉应力的作用下被撕开,从而形成液化裂纹。

2.2 孔隙缺陷的产生机理

增材制造过程中会产生大量不同类型的孔隙缺陷,未熔合孔是其中较常见的一种。未熔合孔主要是由于成型过程中输入的能量不足,粉末材料的熔融不完全或所形成的熔融金属重叠不足^[12,37-38]。当激光能量输入不足时,熔池宽度较窄,无法形成良好的重叠,相邻扫描线之间存在大量未熔化的颗粒;而在后一层

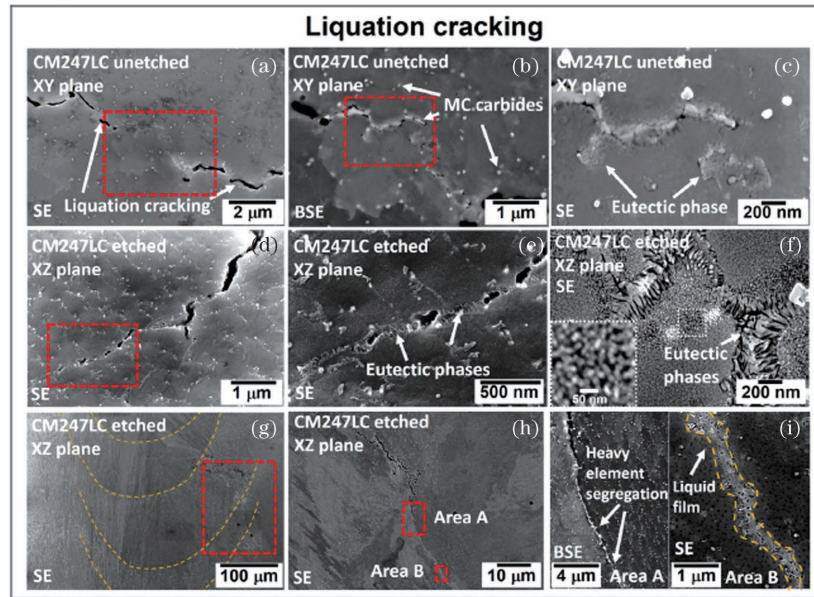


图 2 CM247LC 合金中的液化裂纹^[27]。(a)~(c)未经蚀刻的情况;(d)~(i)蚀刻的情况

Fig. 2 Liquation cracks in CM247LC alloy^[27]. (a)–(c) Without etching; (d)–(i) with etching

的沉积过程中,如果能量输入保持不变,则难以熔化扫描线之间的残留粉末,从而形成较大的孔缺陷;如果能量输入不足导致熔池深度不足,则难以在各层之间形成紧密的重熔,致使形成大的层间未熔合缺陷。Liu

等^[37]在 TC4 合金激光增材制造过程中发现,在未熔合的孔缺陷处,缺陷表面熔融金属的质量和流动性较差,后续沉积易导致缺陷逐渐向上扩展,形成大规模的穿层缺陷,如图 3 所示。

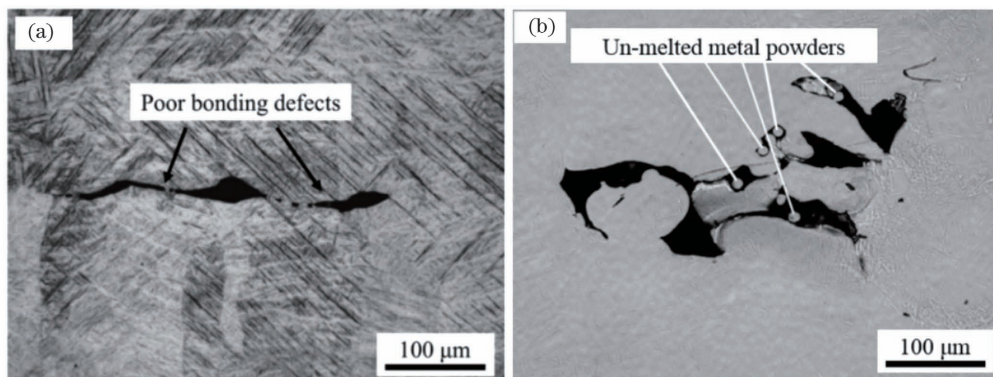


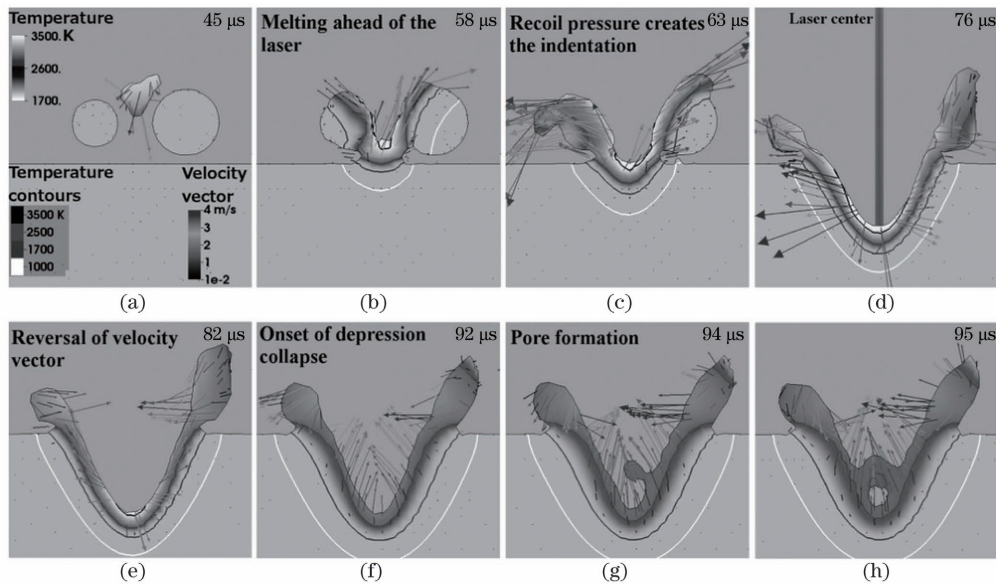
图 3 TC4 合金中的未熔合缺陷^[37]。(a)结合不良缺陷;(b)未熔合孔洞缺陷

Fig. 3 Unfused defects in TC4 alloy^[37]. (a) Poor-bonding defect; (b) unfused hole defect

另一种金属激光增材制造常见孔隙缺陷是气孔。气孔通常形状规则,尺寸较小,其形成原因是气体残留在熔池内部,与熔体流动行为密不可分,可根据来源分为冶金气孔和基于工艺参数的气孔。

冶金气孔是金属粉末包含气体、熔池对气体的吸收等导致的。在等离子雾化等常用粉末冶金法中,气体可能被包裹在液滴中,若气体在凝固过程中不能逸出,就会形成中空粉末;在激光增材制造过程中,粉末熔化,其中的原始气体会保留在熔池中,由于熔池的凝固速度大于气体的逃逸速度,因此熔池中往往会造成规则的圆形孔隙^[39]。熔池吸收气体的具体机制仍未定论,主要为对周围环境气体(氮、氧和氢)的吸收以及某些合金元素的蒸发。前者是在激光增材制造过程中,受表面效应、Marangoni 对流效应、反冲压力效应的综合作用,熔池中部分熔体闭合,进而捕获周围气

体,形成气孔缺陷,如图 4 所示^[40]。研究者制作了激光移出平面时固定位置的轨迹横截面的时间序列模型,用一个逆时针方向循环的速度矢量场表征熔池涡流的运动,温度降低引起 Marangoni 对流,当熔池的表面张力与保持涡流凹陷的反冲力平衡时,该速度矢量场开始反转,这种快速流动可以捕获气体,孔聚集产生更大的孔,最终固化并将气体封闭,形成永久气孔。后者是金属蒸发形成强大的反冲动力,导致熔池中形成匙孔,匙孔不稳定,最终捕获气体形成气孔。Zhao 等^[41]在研究中发现,气孔与匙孔凹陷有关,严重的匙孔不稳定性会导致熔池中产生声波,从而为匙孔尖端附近的孔洞提供额外的驱动力来捕获气体形成气孔;而在某些激光条件下,匙孔壁不断波动和坍塌,表面深匙孔凹陷的快速形成和坍塌会使惰性保护气体氩被困在凝固的金属中,最终形成气孔。

图 4 模拟的 316L 合金中涡流引发气孔的示意图^[40]Fig. 4 Schematic of vortex induced pores in 316L alloy by simulation^[40]

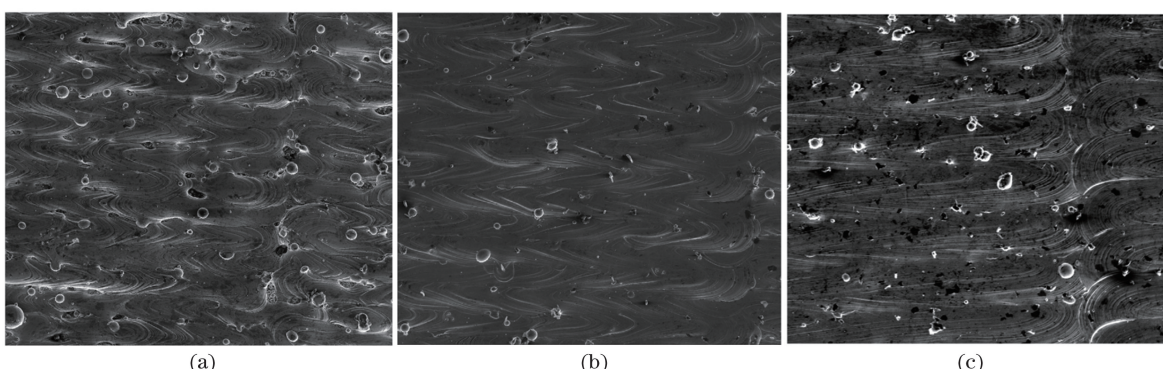
另一种在激光增材制造中产生的常见气孔是工艺参数选用不合理所引起的气孔^[42],主要的影响参数为激光功率和扫描速度。激光功率能够影响能量密度,能量密度计算公式^[43]为

$$E = P / (VD), \quad (1)$$

式中: E 为能量密度; P 为激光功率; V 为扫描速度; D 为光斑直径。

故在相同的扫描速度下,激光功率越高,量密度越高;随着激光功率的增加,熔池会经历不完全熔化、完全熔化、过度熔化等三种状态:激光功率低时能量密度低,粉末层不完全熔化,由于表面张力效应,在层间和熔池内部容易形成平均尺寸较大的孔隙;激光功率适当时能量输入足够,熔池完全熔化,可以形成致密度很高的无孔构件;激光功率大时能量密度高,熔池处于过热状态,Marangoni 对流效应和反冲压力效应增强,温差引起蒸发增强,导致气体圈闭合,形成平均尺寸较小的

孔。Gong 等^[44]利用激光选区熔化技术制备 TC4 合金,通过改变工艺参数,故意制备含气孔的样品,研究结果显示,随着激光功率的增加,孔隙率先减小后增大,如图 5 所示。扫描速度同样可以影响能量密度,进而影响气孔密度,同时还直接影响熔池宽度和深度:扫描速度较大时熔池宽度较宽,扫描速度较小时熔池深度较深。熔池形状的变化会引起熔池中流动模式的改变,进而影响气孔形状。Panwisawas 等^[45]利用激光选区熔化技术制备 TC4,研究了扫描速度与气孔的关系,结果表明,随着激光扫描速度的增加,孔的形状由近球形变为细长形。这是因为随着扫描速度的增加,熔池中的流动模式发生变化:激光束开始扫描时,液气界面分布着紧密的金属粉末,随着激光束的移动,熔池前端回流,尾部流动方向一般是向上的,流速大小接近扫描速度,可将气液界面抬升;当扫描速度过高时,会在扫描轨迹基部附近形成具有不同纵横比且取向与扫描方向不同的孔隙。

图 5 不同激光功率下制备的 TC4 试样^[44]。(a) 80 W;(b) 120 W;(c) 160 WFig. 5 TC4 samples prepared at different laser powers^[44].(a) 80 W; (b) 120 W; (c) 160 W

2.3 夹杂缺陷的产生机理

金属构件激光增材制造过程中产生的夹杂缺陷主要是氧化物夹杂和高熔点金属夹杂^[46-48],其尺度可能从几微米(如高熔点金属夹杂)到几厘米(如氧化物夹

杂,可视),既可属于微观缺陷又可属于宏观缺陷。

氧化物夹杂是指基体中包含与周围组织有所区别的氧化物组织^[46],形态一般为月牙形,常为包含未熔合粉末颗粒及氧化物的黑白相交的组织^[47],图 6 所示

就是常见的氧化物夹杂形貌。其产生原因主要是生产气氛中混入了一定比例的氧气,但具体机理与合金组分有关。高翔宇等^[49]在研究 TC4 合金时发现,当熔覆环境含有氧气时,合金熔滴表面氧化反应生成的氧化皮夹杂嵌入基体,从而对构件质量产生影响;同时氧化物聚集会阻碍熔融合金的熔合,进而形成夹杂物孔洞。张欣^[50]在研究激光直接沉积 24CrNiMoY 合金钢缺陷时发现,当 B、Si 等元素在极快的冷却过程中不能及时浮出逃逸且保护气体失效时,粉末材料成分被氧化,形成氧化物夹杂缺陷。

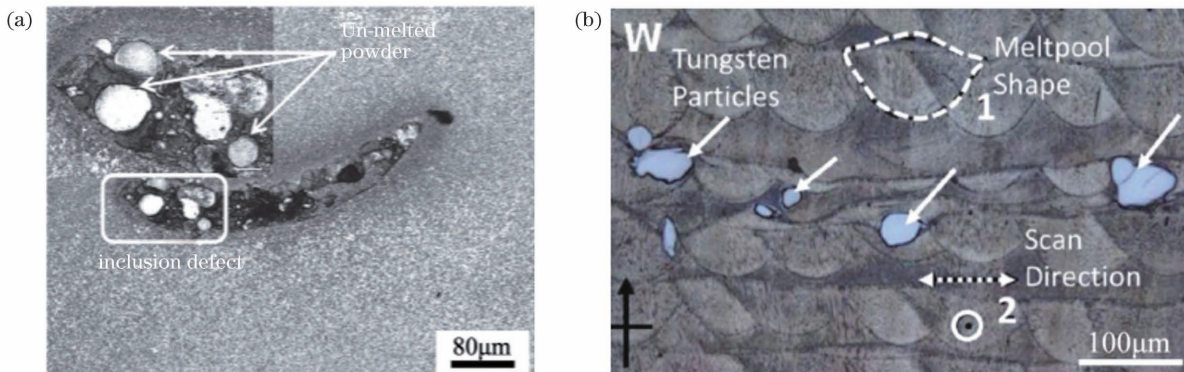


图 6 夹杂缺陷的显微图像。(a) 24CrNiMo 合金样品中的氧化物夹杂^[47]; (b) Inconel625 合金样品中的高熔点钨金属颗粒夹杂^[52]

Fig. 6 Micrographs of inclusion defects. (a) Oxide inclusions in 24CrNiMo alloy sample^[47]; (b) high melting point tungsten particle inclusions in Inconel625 alloy samples^[52]

3 控制金属构件激光增材制造缺陷产生的措施

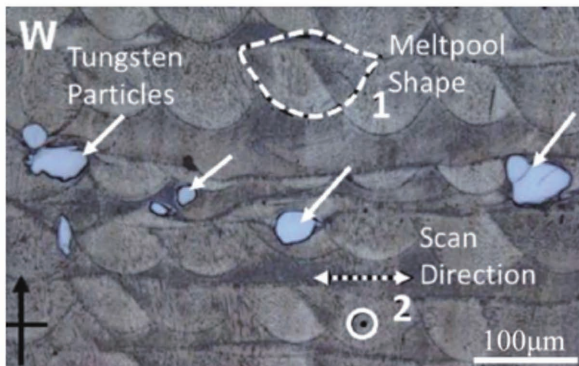
金属构件激光增材制造过程中产生的缺陷将极大影响金属构件的力学性能,甚至导致材料失效,影响其应用,因此应采取适当的控制措施。针对不同类型的合金和缺陷,需采取不同方法,下面将对目前研究及生产中的控制方法进行介绍,并对未来发展方向进行展望。

3.1 裂纹缺陷的控制机制

针对冷裂纹,目前常用的控制方法有优化母材、应急后热等。对于冷裂敏感系数低的材料如钢,应该选择碳当量较低的钢材,减小淬硬倾向^[53-55]。冷裂纹存在潜伏期,一般在制备一段时间后产生,在冷裂纹产生之前及时进行加热处理,也能达到防止裂纹产生的目的^[19]。

针对热裂纹,目前常用的控制方法有优化母材、选取合适加工工艺等。通过优化母材的措施来控制凝固裂纹,应提升液态合金的流动性,缩小凝固区间。Montero-Sistiaga 等^[56]发现,在铝合金中加入适量的 Si 元素,能降低合金的熔点,提高液态合金的流动性,有效防止裂纹的形成和扩展。为了控制液化裂纹,应阻止晶界液化。对于镍基高温合金而言,B、C、P、S 等微量元素在树枝晶间或晶界的富集将大大提高低熔点共晶物相的含量,导致热裂纹的形成^[57-60],因此应控制

高熔点金属夹杂是指金属构件中夹杂了与基体材料成分不同的高密度高熔点金属如 W、Mo 等,这种夹杂形态可为颗粒状和块状。这类缺陷产生的原因一般有两类。一类是由于高熔点金属难熔。例如文艺^[51]在研究激光快速成型两相钛合金内部 W 夹杂的实验中发现,W 颗粒熔点极高而未发生明显熔化变形,因此 W 颗粒基本以原有形貌嵌入到基体中;Montazeri 等^[52]在制备的 Inconel625 中发现了金属钨颗粒夹杂,如图 6 所示。另一类是粉末颗粒原料受到污染,这可能是制备过程受到污染或者制粉过程中操作不当引起的。



其添加量;对于铝合金而言,包括 Al-Cu 系、Al-Mg 系和 Al-Zn 系,在激光增材制造过程中热裂倾向严重,有研究^[61]表明,在铝合金内少量地添加 Y₂O₃ 可以有效地减少微量元素的富集,净化晶界,抑制激光增材制造过程中液化裂纹的产生。在加工过程中也应采取适当的措施来减少裂纹,常用的措施有三种。

1)选择合适的工艺参数。根据式(1)可知,增加激光功率和降低扫描速度可以增大激光功率密度,从而减小熔池的温度梯度,降低冷却速度,增加冷却时间,减少凝固收缩带来的应力,增强熔池的回填作用,抑制裂纹的产生。Chen 等^[26]发现,在激光增材制造 Inconel718 时,提升激光功率或降低扫描速度可以减少高温合金的裂纹数量,减小开裂倾向,如图 7 所示。多名学者的研究^[62-63]也都给出了类似的规律。Zhang 等^[64]更是根据弗雷尔标准进行裂纹敏感性分析,给出了铝合金凝固裂纹产生的临界扫描速度。

2)预热。热应力是导致材料开裂的主要因素之一,这种由温度变化引起的应力计算公式为

$$\alpha = E' \alpha_1 (T_0 - T_f) = E \alpha_1 \Delta T, \quad (2)$$

式中:E' 为弹性模量;α 为线性热膨胀系数;T_f 为基板表面温度;T₀ 为材料内部温度;ΔT 为降温过程中材料内部的温度梯度,材料的热应力正比于其内部的温度梯度。

预热的主要目的是降低沉积过程中的温度梯度,减缓冷却速度,能够更大程度地释放热应力,从而避免

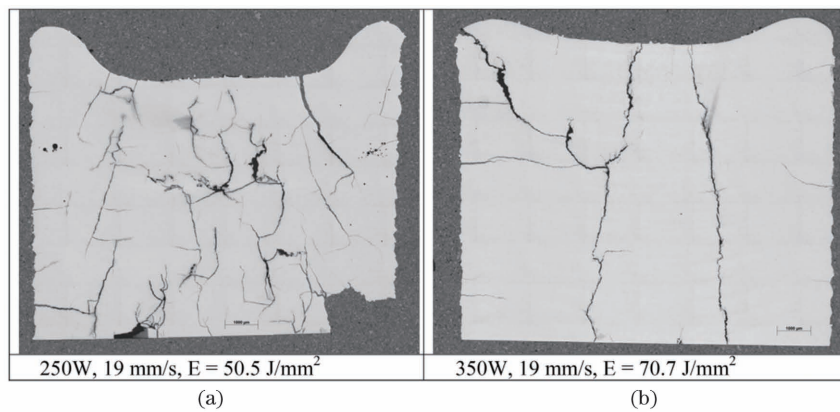


图 7 不同激光功率密度下激光增材制造 Inconel718 高温合金的宏观形貌^[26]。(a) 50.5 J/mm^2 ; (b) 70.7 J/mm^2

Fig. 7 Macroscopic morphologies of Inconel718 superalloy prepared at different laser power densities^[26]. (a) 50.5 J/mm^2 ; (b) 70.7 J/mm^2

热裂纹的产生。Tang 等^[65]发现,对基材进行预热并在每一层沉积之前都进行预热,如图 8 所示,相比于中间过程未进行预热,所得的试样具有更低的位错密度,揭示预热实质是应力释放过程。Brückner 等^[66]对裂纹敏感性材料 Ni 基高温合金以及 TiAl 进行了激光增

材制造,通过热成像技术的辅助,将温度控制在一定范围内可以控制裂纹的产生。Jendrzejewski 等^[67-69]在 SF6 合金的激光增材制造过程中发现,基体预热至 750 K 时,合金的裂纹显著减少,当预热温度达到 950 K 时,可以完全消除合金中的裂纹。

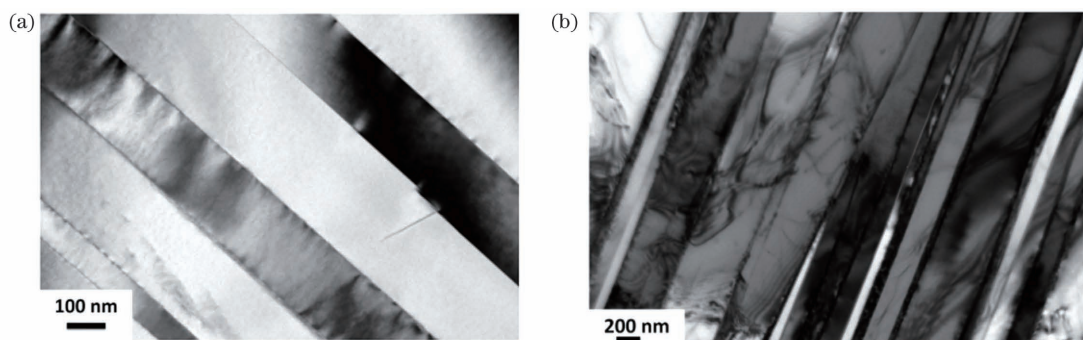


图 8 不同热处理条件下的高透射电镜明场像照片^[65]。(a)每层沉积过程都经预热处理;(b)中间沉积过程未经预热处理

Fig. 8 High transmission electron microscope bright field images under different heat treatment conditions^[65]. (a) When each layer is preheated in deposition process; (b) when intermediate deposition process is not preheated

3)选取适合的工艺手段。激光入射角和扫描路径等都会对构件成型情况产生影响。Chen 等^[58]研究表明,当改变激光入射角使得激光能量更多地会聚于熔池前端时,熔池的侧向散热得到增强,促进了激光增材制造 Inconel 718 合金内部树枝晶间的二次树枝晶的生长,形成了许多规则的交错带组织,从而避免了长链状低熔点共晶 Laves 相的形成,增强了树枝晶之间的连接,从而提高了合金热裂纹萌生与扩展的阻力。Wang^[70]利用激光选区熔化技术制备 Mo 合金时,设置了分层旋转扫描方式,从而形成了互锁晶界结构,增加了制备过程中裂纹扩展的阻力,减少了制备过程中裂纹的产生。此外,Sharman 等^[63,71]发现,沉积平面上的散焦激光会使粉末在送粉过程中提前熔化,减小了冷却速度,降低了温度梯度,致使开裂临界值升高,裂纹减少。除了上文提到的这些手段外,还可以通过添加支撑和激光重熔等手段来抑制裂纹。Wang 等^[70,72]的研究表明,在激光选区熔化(SLM)金属构件制备过程中,适当添加支持可以有效减小零件与基板

间的接触面积,散热能力减弱,从而延长凝固时间,降低冷却速率和零件内部的温度梯度,从而减小热应力,抑制裂纹形成。邓国威等^[72]的研究表明,适当使用激光重熔可以有效抑制裂纹的形成,不同的重熔参数对裂纹抑制效果不同。

3.2 孔隙缺陷的控制机制

为了控制孔隙缺陷,应从粉材制备、工艺参数控制及后处理入手。

不同合金对孔隙的敏感程度不同,可以根据产品需求,适当添加一些合金元素以改变合金成分,使得合金对孔隙缺陷的敏感度下降,从而降低孔隙率;同时,合理地改善粉末质量可以有效减小孔隙率,例如在粉末进入仪器之前进行干燥处理^[73]。

调整合适的工艺参数也能降低孔隙率。在李永涛^[10]的研究中,钛合金增材制造零件的孔隙率与激光功率、扫描速度、扫描间距和舱口间距有关,调整各参数可以有效降低孔隙率。如图 9 所示,Kasperovich 等^[74]的研究也表明,在一定范围内调整

扫描速度和激光功率可以降低孔隙率;且由于孔隙会不可避免地出现,可以采用稍微增加功率密度的方法,使球形孔代替尖锐的未熔合孔,适当缓解应力。

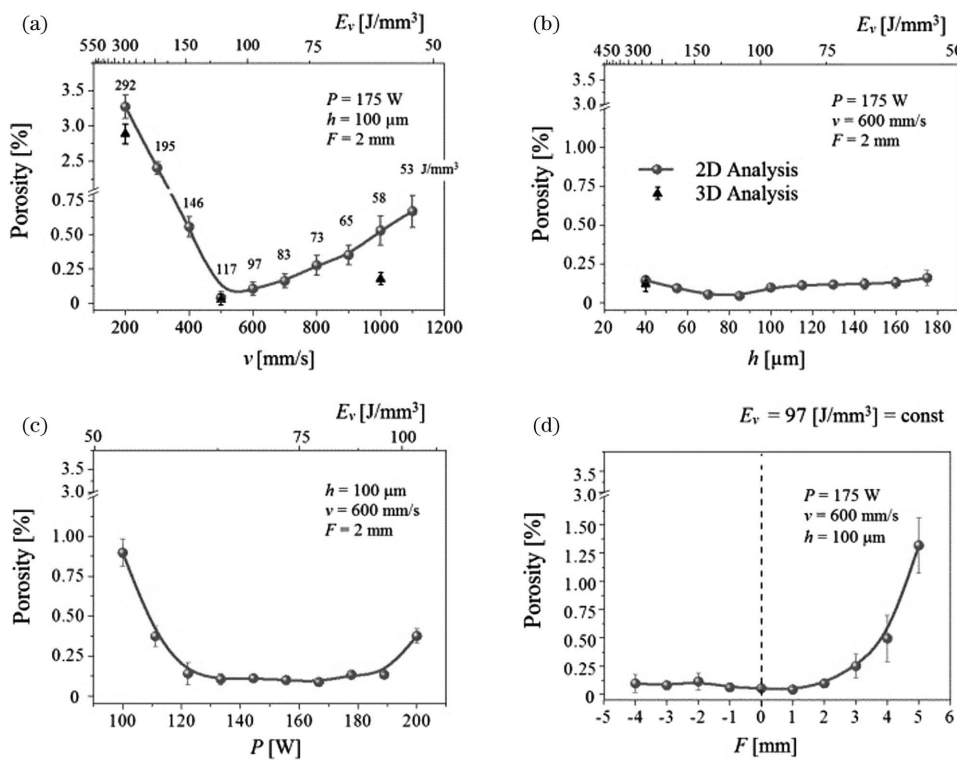


图 9 工艺参数对孔隙率的影响^[74]。(a) 扫描速度; (b) 扫描间距; (c) 激光功率; (d) 舱口间距

Fig. 9 Influence of each process parameter on porosity^[74]. (a) Scanning speed; (b) scanning spacing; (c) laser power; (d) hatch spacing

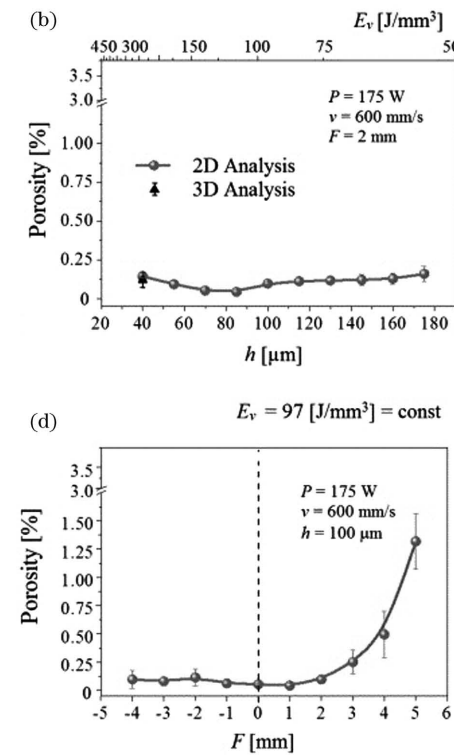
与常规零件类似,后处理可以明显提升增材制造零件的性能^[76]。热等静压处理(HIP)可以显著减小孔隙率^[77],即在惰性气体氛围下同时对零件进行高温和高压处理,高温导致屈服强度降低和扩散率提高,高压导致小规模的塑性流动,最终使孔塌陷。HIP 可显著减少孔隙的数量,恢复微观结构^[78-80]。Zhou 等^[81]在真空中生产 SLM 样品时,发现 HIP 将孔隙率从 0.095% 降低至 0.067% (HIP) 和 0.044% (HIP 后又进行热处理)。Chen 等^[82]对复杂的 L-PBF Ti6-Al4-Vb 胞状结构进行了 HIP,消除了预制柱中 0.5% (体积分数) 的孔。Tammam-Williams 等^[83]的研究证实,HIP 会使得较大的未熔合孔封闭,但无法消除所有孔隙。

3.3 夹杂缺陷的控制机制

夹杂的存在会对构件性能产生较大影响,均匀分布的细小夹杂会产生弥散强化的作用,因此需要控制的是颗粒较大的夹杂。

对于高熔点金属夹杂缺陷来说,有效的控制手段有设置合理的工艺参数和扫描模式及减少烟尘产生。高熔点金属颗粒较难熔化,设置合理的工艺参数可以减少未熔化颗粒夹杂,同时不诱发其他类型的缺陷。张欣^[50]对 24CrNiMoY 合金钢进行了激光直接沉积,发现制备过程中能量输入不足导致粉末熔化不充分,在夹杂缺陷处发现较多未熔化的粉末颗粒。张晓丽

集中现象。Martin 等^[75]研究发现,可以通过适当调节激光功率来避免熔池过热,减小激光转折处的孔隙率。



等^[84]研究了激光选区熔化 AlSi12 试样工艺参数对致密度的影响,结果表明,当工艺参数选择不当时,成型层表面质量将会受到影响。选用合理的扫描方式可以扩大重熔区域,降低高熔点金属不熔的概率。研究者采用不同的扫描方式制备 AlSi10Mg 成型样件,结果表明,当采用单向扫描和“之”字形扫描时,起始端和末端的激光功率不稳定,扫描速度较低,能量输入较高,导致熔池不稳定,极易产生夹杂及其他缺陷;当采用同向扫描方式进行重熔时,球化和搭接不均匀等问题得到解决;当采用旋转 90° 的扫描方式进行重熔时,成型件表面整洁、杂质较少,成型件致密度得到提高。在增材制造过程中,可能会出现烟尘,从而导致夹杂的产生。张晓丽等^[84]研究发现,加入 Fe_2O_3 后,制造过程中的发尘量减小,焊缝中夹杂物的尺寸和数量均有所减小;改变保护气体的流速和压力也会减少烟尘,从而控制夹杂物的数量,但目前关于增材制造过程中烟尘以及气体流量对夹杂的影响研究较少,未来可进行更深入的研究。

对于氧化物夹杂缺陷来说,主要的控制方法是控制加工环境中的氧含量。黄煜华^[85]为了研究 Ti 和 Al 氧化物的夹杂现象,设计了低氧环境与正常环境下的对比实验,发现降低氧含量时,激光增材制造过程中的成型件质量和精度均得到了极大的提高;同时,低氧

环境下成型件的抗拉强度明显高于正常环境下的。

4 结束语

金属构件的激光熔化沉积增材制造技术是一种高性能、低成本、可设计的制造技术,此技术可实现难熔、难加工、高活性金属材料的快速、低成本、高精度成型制备。但是,关于复杂应力交互作用和熔池熔体流动等对零件变形失效的影响仍缺乏深入研究,缺陷导致材料性能降低仍然是制约激光增材制造技术发展的难题之一。为了实现激光增材制造过程中缺陷的有效控制,解决金属构件激光增材制造和使用过程中与缺陷相关的问题,可从以下四个方面进行更加深入的研究。

1) 针对裂纹缺陷,探讨不同工艺条件下激光增材制造过程中的应力演化规律和零件失效行为与复杂应力和熔体流动耦合作用之间的联系。

2) 针对孔隙缺陷,探讨各项参数对缺陷影响的量化关系及孔隙产生与熔体凝固和气体逸出等之间的联系。

3) 针对夹杂缺陷,探讨增材制造过程中保护气氛气体成分和流量影响缺陷产生的热力学机理。

4) 针对上述几种缺陷,探讨高温度梯度、高冷却速度下非平衡凝固材料的缺陷控制新方法。

参 考 文 献

- [1] 王华明. 飞机钛合金大型构件激光成形工艺与装备[J]. 中国科技成果, 2014, (11): 17, 20.
Wang H M. Laser forming technology and equipment for large aircraft titanium alloy components [J]. Chinese scientific and technological achievements , 2014, (11): 17, 20.
- [2] 杨德建, 刘仁洪. 大型复杂金属零件 3D 打印技术及研究进展[J]. 兵工自动化, 2017, 36(2): 8-12.
Yang D J, Liu R H. Research development of 3D printing for large complex metal parts[J]. Ordnance Industry Automation, 2017, 36(2): 8-12.
- [3] 赵建仓, 朱平, 李清海. 核电大型构件关键焊接技术[J]. 金属加工(热加工), 2012(12): 18-22.
Zhao J C, Zhu P, Li Q H. Key welding technology of large nuclear power components[J]. MW Metal Forming, 2012(12): 18-22.
- [4] 王华明. 高性能大型金属构件激光增材制造:若干材料基础问题[J]. 航空学报, 2014, 35(10): 2690-2698.
Wang H M. Materials' fundamental issues of laser additive manufacturing for high-performance large metallic components [J]. Acta Aeronautica et Astronautica Sinica, 2014, 35(10): 2690-2698.
- [5] Emmelmann C, Sander P, Kranz J, et al. Laser additive manufacturing and bionics: redefining lightweight design [J]. Physics Procedia, 2011, 12: 364-368.
- [6] Gu D D. Laser additive manufacturing of high-performance materials[M]. Heidelberg: Springer, 2015.
- [7] 林鑫, 黄卫东. 高性能金属构件的激光增材制造[J]. 中国科学:信息科学, 2015, 45(9): 1111-1126.
Lin X, Huang W D. Laser additive manufacturing of high-performance metal components [J]. Scientia Sinica (Informationis), 2015, 45(9): 1111-1126.
- [8] 卢秉恒, 李涤尘. 增材制造(3D打印)技术发展[J]. 机械制造与自动化, 2013, 42(4): 1-4.
Lu B H, Li D C. Development of the additive manufacturing(3D printing) technology [J]. Machine Building & Automation, 2013, 42(4): 1-4.
- [9] 于梦晓, 李佳, 李卓, 等. 热处理对激光增材制造 AerMet100 超高强度钢动态力学性能的影响[J]. 中国激光, 2020, 47(11): 1102003.
Yu M X, Li J, Li Z, et al. Effect of heat treatment on dynamic mechanical properties of AerMet100 ultrahigh strength steel fabricated by laser additive manufacturing [J]. Chinese Journal of Lasers, 2020, 47(11): 1102003.
- [10] 李永涛. 钛合金激光增材制造缺陷研究[D]. 大连: 大连理工大学, 2017.
Li Y T. The study on defect formation in laser additive manufacturing titanium alloy [D]. Dalian: Dalian University of Technology, 2017.
- [11] 陈滋鑫, 周后明, 徐采星. 激光熔覆裂纹研究现状[J]. 激光与光电子学进展, 2021, 58(7): 0700006.
Chen Z X, Zhou H M, Xu C X. Cladding crack in laser cladding: a review [J]. Laser & Optoelectronics Progress, 2021, 58(7): 0700006.
- [12] Li R D, Liu J H, Shi Y S, et al. 316L stainless steel with gradient porosity fabricated by selective laser melting [J]. Journal of Materials Engineering and Performance, 2010, 19(5): 666-671.
- [13] Aboulkhair N T, Everitt N M, Ashcroft I, et al. Reducing porosity in AlSi₁₀Mg parts processed by selective laser melting [J]. Additive Manufacturing, 2014, 1/2/3/4: 77-86.
- [14] Gu D D, Hagedorn Y C, Meiners W, et al. Densification behavior, microstructure evolution, and wear performance of selective laser melting processed commercially pure titanium[J]. Acta Materialia, 2012, 60(9): 3849-3860.
- [15] Gong H, Rafi H K, Nadimpalli K, et al. Defect morphology in Ti-6Al-4V parts fabricated by selective laser melting and electron beam melting [EB/OL]. [2021-05-06]. <https://repositories.lib.utexas.edu/handle/2152/88632>.
- [16] Harrison N J, Todd I, Mumtaz K. Reduction of micro-cracking in nickel superalloys processed by Selective Laser Melting: a fundamental alloy design approach[J]. Acta Materialia, 2015, 94: 59-68.
- [17] 赵官源, 王东东, 白培康, 等. 铝合金激光快速成型技术研究进展[J]. 热加工工艺, 2010, 39(9): 170-173, 177.
Zhao G Y, Wang D D, Bai P K, et al. Research progress of laser rapid prototyping technology for aluminum alloy[J]. Hot Working Technology, 2010, 39(9): 170-173, 177.
- [18] 王浩舟. 焊接冷裂纹成因及预防研究[J]. 城市建设理论研究(电子版), 2015, 5(12): 2089-2090.
Wang H Z. Study on Causes and prevention of welding cold crack[J]. ChengShi Jianshe LiLun Yan Jiu, 2015, 5(12): 2089-2090.
- [19] 罗伟中. 低合金高强钢焊接冷裂纹研究[J]. 焊接研究与生产, 1994(2): 29-32.
Luo W Z. Study on welding cold crack of low alloy high strength steel. Welding Research and Production, 1994(2): 29-32.
- [20] 杨建国, 黄鲁永, 张勇, 等. 30CrMnSi 钢 TIG 焊冷裂纹形成机制[J]. 焊接学报, 2011, 32(12): 13-16, 113.
Yang J G, Huang L Y, Zhang Y, et al. Mechanism of cold welding cracks in 30CrMnSi steel joints welded by TIG method [J]. Transactions of the China Welding Institution, 2011, 32(12): 13-16, 113.
- [21] 汪辉, 卜华全, 房务农. NK-HITEN610U2L 钢板焊接冷裂纹敏感性[J]. 石油化工设备, 2006, 35(4): 13-16.
Wang H, Bu H Q, Fang W N. Study on welding cold-sensible crack of NK-HITEN610U2L steel [J]. Petro-Chemical Equipment, 2006, 35(4): 13-16.
- [22] Chen Y H. Preventing technique of welding cold cracking[J]. Technological Development of Enterprise, 2006, 25(7): 54-55.
- [23] Kempen K, Vrancken B, Buls S, et al. Selective laser melting of crack-free high density M2 high speed steel parts by baseplate preheating [J]. Journal of Manufacturing Science and Engineering, 2014, 136(6): 061026.

- [24] Idowu O A, Ojo O A, Chaturvedi M C. Effect of heat input on heat affected zone cracking in laser welded ATI Allvac 718Plus superalloy [J]. Materials Science and Engineering: A, 2007, 454/455: 389-397.
- [25] Zhong M L, Sun H Q, Liu W J, et al. Boundary liquation and interface cracking characterization in laser deposition of Inconel 738 on directionally solidified Ni-based superalloy [J]. Scripta Materialia, 2005, 53(2): 159-164.
- [26] Chen Y, Zhang K, Huang J, et al. Characterization of heat affected zone liquation cracking in laser additive manufacturing of Inconel 718 [J]. Materials & Design, 2016, 90: 586-594.
- [27] Tang Y T, Panwisawas C, Ghoussoub J N, et al. Alloys-by-design: application to new superalloys for additive manufacturing [J]. Acta Materialia, 2021, 202: 417-436.
- [28] Eskin D G, Katgerman L. A quest for a new hot tearing criterion [J]. Metallurgical and Materials Transactions A, 2007, 38(7): 1511-1519.
- [29] 王小杰. Al-Mg-Si合金激光焊接凝固裂纹形成机理研究 [D]. 上海: 上海交通大学, 2015.
- Wang X J. Formation mechanism of solidification cracking in laser welding on Al-Mg-Si alloy [D]. Shanghai: Shanghai Jiao Tong University, 2015.
- [30] 于汉臣, 闫涵, 栾天曼, 等. 紫铜厚板 GTAW 热裂纹形成原因分析 [J]. 焊接学报, 2018, 39(8): 87-91, 133.
- Yu H C, Yan H, Luan T M, et al. Investigation on the cause of the hot cracking in GTA welding of thick copper plates [J]. Transactions of the China Welding Institution, 2018, 39(8): 87-91, 133.
- [31] Stangeland A, Mo A, M'Hamdi M, et al. Thermal strain in the mushy zone related to hot tearing [J]. Metallurgical and Materials Transactions A, 2006, 37(3): 705-714.
- [32] Rapaz M, Drezen J M, Mathier V, et al. Towards a micro-macro model of hot tearing [J]. Materials Science Forum, 2006, 519/520/521: 1665-1674.
- [33] de Lima M S F. Phase transformations during laser processing of aerospace metallic materials [J]. Advanced Materials Research, 2016, 1135: 179-201.
- [34] Wang X J, Lu F G, Wang H P, et al. Mechanical constraint intensity effects on solidification cracking during laser welding of aluminum alloys [J]. Journal of Materials Processing Technology, 2015, 218: 62-70.
- [35] Langlais J, Gruzleski J E. A novel approach to assessing the hot tearing susceptibility of aluminium alloys [J]. Materials Science Forum, 2000, 331/332/333/334/335/336/337: 167-172.
- [36] Lippold J C. Heat-affected zone liquation cracking in austenitic and duplex stainless steels [J]. Welding Journal, 1992: 71.
- [37] Liu Q C, Elambasseril J, Sun S J, et al. The effect of manufacturing defects on the fatigue behaviour of Ti-6Al-4V specimens fabricated using selective laser melting [J]. Advanced Materials Research, 2014, 891/892: 1519-1524.
- [38] Vilari T, Colin C, Bartout J D. As-fabricated and heat-treated microstructures of the Ti-6Al-4V alloy processed by selective laser melting [J]. Metallurgical and Materials Transactions A, 2011, 42(10): 3190-3199.
- [39] 房冬青, 严振宇, 黄超, 等. 5056铝合金激光-TIG电弧复合焊接接头气孔特性的研究 [J]. 电加工与模具, 2015(5): 52-53, 57.
- Fang D Q, Yan Z Y, Huang C, et al. Study on pore characteristics of 5056 aluminum alloy joints welded by laser-TIG hybrid [J]. Electromachining & Mould, 2015(5): 52-53, 57.
- [40] Khairallah S A, Anderson A T, Rubenchik A, et al. Laser powder-bed fusion additive manufacturing: physics of complex melt flow and formation mechanisms of pores, spatter, and denudation zones [J]. Acta Materialia, 2016, 108: 36-45.
- [41] Zhao C, Parab N D, Li X X, et al. Critical instability at moving keyhole tip generates porosity in laser melting [J]. Science, 2020, 370(6520): 1080-1086.
- [42] Gong H, Gu H, Zeng K, et al. Melt pool characterization for selective laser melting of Ti-6Al-4V pre-alloyed powder [EB/OL]. [2021-06-03]. <https://repositories.lib.utexas.edu/handle/2152/88748>.
- [43] Read N, Wang W, Essa K, et al. Selective laser melting of AlSi₁₀Mg alloy: process optimisation and mechanical properties development [J]. Materials & Design, 2015, 65: 417-424.
- [44] Gong H J, Rafi K, Gu H F, et al. Analysis of defect generation in Ti-6Al-4V parts made using powder bed fusion additive manufacturing processes [J]. Additive Manufacturing, 2014, 1/2/3/4: 87-98.
- [45] Panwisawas C, Qiu C L, Sovani Y, et al. On the role of thermal fluid dynamics into the evolution of porosity during selective laser melting [J]. Scripta Materialia, 2015, 105: 14-17.
- [46] 郭政亚, 熊振华. 金属增材制造缺陷检测技术 [J]. 哈尔滨工业大学学报, 2020, 52(5): 49-57.
- Guo Z Y, Xiong Z H. Defect detection technology in metal additive manufacturing [J]. Journal of Harbin Institute of Technology, 2020, 52(5): 49-57.
- [47] Cao L, Chen S Y, Wei M W, et al. Effect of laser energy density on defects behavior of direct laser depositing 24CrNiMo alloy steel [J]. Optics & Laser Technology, 2019, 111: 541-553.
- [48] 冯涛. 论固体夹杂的分类与特点 [J]. 职业, 2014(12): 157.
- Feng T. On the classification and characteristics of solid inclusions [J]. Occupation, 2014(12): 157.
- [49] 高翔宇, 高祥熙, 姜涛, 等. 增材制造大型钛合金横梁缺陷分析 [J]. 失效分析与预防, 2018, 13(1): 43-48.
- Gao X Y, Gao X X, Jiang T, et al. Defects analysis of large additive manufacturing beam of titanium alloy [J]. Failure Analysis and Prevention, 2018, 13(1): 43-48.
- [50] 张欣. 激光直接沉积 24CrNiMoY 合金钢缺陷研究 [D]. 沈阳: 沈阳师范大学, 2020.
- Zhang X. Study on defects of laser direct deposition of 24CrNiMoY alloy steel [D]. Shenyang: Shenyang Normal University, 2020.
- [51] 文艺. 3D 打印两相钛合金组织特征及缺陷研究 [D]. 南昌: 南昌航空大学, 2016.
- Wen Y. Research on microstructure and defects of two-phase titanium alloy with 3D printing [D]. Nanchang: Nanchang Hangkong University, 2016.
- [52] Montazeri M, Yavari R, Rao P, et al. In-process monitoring of material cross-contamination defects in laser powder bed fusion [J]. Journal of Manufacturing Science and Engineering, 2018, 140(11): 111001.
- [53] Järvinen J P, Matilainen V, Li X Y, et al. Characterization of effect of support structures in laser additive manufacturing of stainless steel [J]. Physics Procedia, 2014, 56: 72-81.
- [54] de Lima M S F, Sankaré S. Microstructure and mechanical behavior of laser additive manufactured AISI 316 stainless steel stringers [J]. Materials & Design, 2014, 55: 526-532.
- [55] Riemer A, Leuders S, Thöne M, et al. On the fatigue crack growth behavior in 316L stainless steel manufactured by selective laser melting [J]. Engineering Fracture Mechanics, 2014, 120: 15-25.
- [56] Montero-Sistiaga M L, Mertens R, Vrancken B, et al. Changing the alloy composition of Al7075 for better processability by selective laser melting [J]. Journal of Materials Processing Technology, 2016, 238: 437-445.
- [57] Idowu O A, Ojo O A, Chaturvedi M C. Crack-free electron beam welding of allvac 718Plus (R) superalloy [J]. Welding Journal, 2009, 88(9): 179S-187S.
- [58] Chen W, Chaturvedi M C, Richards N L. Effect of boron segregation at grain boundaries on heat-affected zone cracking in wrought INCONEL 718 [J]. Metallurgical and Materials Transactions A, 2001, 32(4): 931-939.
- [59] Guo H, Chaturvedi M C, Richards N L. Effect of sulphur on hot ductility and heat affected zone microfissuring in Inconel 718 welds [J]. Science and Technology of Welding and Joining, 2000, 5(6): 378-384.

- [60] Thompson R G, Mayo D E, Radhakrishnan B. The relationship between carbon content, microstructure, and intergranular liquation cracking in cast nickel alloy 718 [J]. Metallurgical Transactions A, 1991, 22(2): 557-567.
- [61] 陈智君, 张群莉, 楼程华, 等. Inconel 738 激光熔覆层的裂纹控制方法[J]. 应用激光, 2013, 33(1): 7-13.
- Chen Z J, Zhang Q L, Lou C H, et al. Methods of crack control for Inconel 738 laser cladding layer[J]. Applied Laser, 2013, 33(1): 7-13.
- [62] Liu W P, DuPont J N. Fabrication of carbide-particle-reinforced titanium aluminide-matrix composites by laser-engineered net shaping[J]. Metallurgical and Materials Transactions A, 2004, 35(13): 1133-1140.
- [63] Sharman A R C, Hughes J I, Ridgway K. Characterisation of titanium aluminide components manufactured by laser metal deposition[J]. Intermetallics, 2018, 93: 89-92.
- [64] Zhang H, Zhu H H, Nie X J, et al. Effect of Zirconium addition on crack, microstructure and mechanical behavior of selective laser melted Al-Cu-Mg alloy[J]. Scripta Materialia, 2017, 134: 6-10.
- [65] Tang H P, Yang G Y, Jia W P, et al. Additive manufacturing of a high niobium-containing titanium aluminide alloy by selective electron beam melting [J]. Materials Science and Engineering: A, 2015, 636: 103-107.
- [66] Brückner F, Finaske T, Willner R, et al. Laser additive manufacturing with crack-sensitive materials[J]. Laser Technik Journal, 2015, 12(2): 28-30.
- [67] Jendrzejewski R, Śliwiński G, Krawczuk M, et al. Temperature and stress fields induced during laser cladding[J]. Computers & Structures, 2004, 82(7/8): 653-658.
- [68] Jendrzejewski R, Śliwiński G. Investigation of temperature and stress fields in laser cladded coatings [J]. Applied Surface Science, 2007, 254(4): 921-925.
- [69] Jendrzejewski R, Śliwiński G, Conde A, et al. Influence of the base preheating on cracking of the laser-cladded coatings [J]. Proceedings of SPIE, 2003, 5121: 356-361.
- [70] Wang D Z, Yu C F, Ma J, et al. Densification and crack suppression in selective laser melting of pure molybdenum[J]. Materials & Design, 2017, 129: 44-52.
- [71] Thomas M, Malot T, Aubry P. Laser metal deposition of the intermetallic TiAl alloy [J]. Metallurgical and Materials Transactions A, 2017, 48(6): 3143-3158.
- [72] 邓国威, 谭超林, 王迪, 等. 增材制造高体积陶瓷增强马氏体钢缺陷抑制与机理研究[J]. 机械工程学报, 2021, 57(17): 243-252.
- Deng G W, Tan C L, Wang D, et al. Defects suppression and mechanism in additive manufacturing high-volume SiC reinforced maraging steel[J]. Journal of Mechanical Engineering, 2021, 57(17): 243-252.
- [73] Li X P, O'Donnell K M, Sercombe T B. Selective laser melting of Al-12Si alloy: enhanced densification via powder drying[J]. Additive Manufacturing, 2016, 10: 10-14.
- [74] Kasperovich G, Haubrich J, Gussone J, et al. Correlation between porosity and processing parameters in $TiAl_6V_4$ produced by selective laser melting[J]. Materials & Design, 2016, 105: 160-170.
- [75] Martin A A, Calta N P, Khairallah S A, et al. Dynamics of pore formation during laser powder bed fusion additive manufacturing[J]. Nature Communications, 2019, 10: 1987.
- [76] 肖来荣, 谭威, 刘黎明, 等. 后处理对增材制造 GH3536 合金组织与性能的影响[J]. 激光与光电子学进展, 2021, 58(17): 1714010.
- Xiao L R, Tan W, Liu L M, et al. Effect of post treatment on the microstructure and properties of the GH3536 alloy formed by additive manufacturing[J]. Laser & Optoelectronics Progress, 2021, 58(17): 1714010.
- [77] Qiu C L, Adkins N J E, Attallah M M. Microstructure and tensile properties of selectively laser-melted and of HIPed laser-melted Ti_6Al_4V [J]. Materials Science and Engineering: A, 2013, 578: 230-239.
- [78] Mower T M, Long M J. Mechanical behavior of additive manufactured, powder-bed laser-fused materials[J]. Materials Science and Engineering: A, 2016, 651: 198-213.
- [79] Kasperovich G, Hausmann J. Improvement of fatigue resistance and ductility of $TiAl_6V_4$ processed by selective laser melting[J]. Journal of Materials Processing Technology, 2015, 220: 202-214.
- [80] Greitemeier D, Palm F, Syassen F, et al. Fatigue performance of additive manufactured $TiAl_6V_4$ using electron and laser beam melting [J]. International Journal of Fatigue, 2017, 94: 211-217.
- [81] Zhou B, Zhou J, Li H X, et al. A study of the microstructures and mechanical properties of Ti_6Al_4V fabricated by SLM under vacuum[J]. Materials Science and Engineering: A, 2018, 724: 1-10.
- [82] Chen J K, Wu M W, Cheng T L, et al. Continuous compression behaviors of selective laser melting $Ti-6Al-4V$ alloy with cuboctahedron cellular structures[J]. Materials Science and Engineering: C, 2019, 100: 781-788.
- [83] Tammas-Williams S, Withers P J, Todd I, et al. Porosity regrowth during heat treatment of hot isostatically pressed additively manufactured titanium components [J]. Scripta Materialia, 2016, 122: 72-76.
- [84] 张晓丽, 齐欢, 魏青松. 铝合金粉末选择性激光熔化成形工艺优化试验研究[J]. 应用激光, 2013, 33(4): 391-397.
- Zhang X L, Qi H, Wei Q S. Experimental study of selective laser melted $AlSi_{12}$ [J]. Applied Laser, 2013, 33(4): 391-397.
- [85] 黄煜华. 18Ni300 激光增材制造工艺及视觉传感研究[D]. 哈尔滨: 哈尔滨工业大学, 2017.
- Huang Y H. Research on 18Ni300 fabricated by laser additive manufacturing and vision sensing[D]. Harbin: Harbin Institute of Technology, 2017.

Review on Defect Formation Mechanisms and Control Methods of Metallic Components During Laser Additive Manufacturing

Yao Xunjie¹, Wang Jiawei¹, Yang Yancheng¹, Zhang Xinyue¹, Cheng Xu^{2*}, Zhang Shuquan³

¹ School of Material Science and Engineering, Beihang University, Beijing 100191, China;

² Research Institute for Frontier Science, Beihang University, Beijing 100191, China;

³ Beijing Yuding Additive Manufacturing Research Institute Co., Ltd., Beijing 100096, China

Abstract

Significance Metallic components have been widely used in aviation, aerospace, marine and other industrial departments for their excellent properties. Over the past decades, metallic components are developing toward to high-

performance and multi-function but with low production cost, which pushes new manufacturing techniques to be used. Laser additive manufacture (LAM) is one of the new additive manufacturing techniques, which is widely used to manufacture near-net-shaped metal parts layer-by-layer by melting metal powders using a laser beam. Now, it is also widely used to manufacture large and critical high performance metallic components with advantages in reducing material waste, production time and cost. In the LAM process, the components undergo periodic and unstable thermal cycling, which influences the microstructure and internal stress. More importantly, the inappropriate selection of process parameters leads to the appearance of defects with degradation of mechanical property. For example, if there exists porosity in the material powder, the pores occur during LAM and the liquid condensation speed is faster than the gas escape speed. If the selected laser power is too low, the powder is hardly fully molten and the unfused pores and inclusions are generated.

Therefore, the extensive researches worldwide focus on studying the generation mechanism of defects in the LAM process. In Deng's research, the 15% (volume fraction) SiC ceramic reinforced steel (MS) metal matrix composites were prepared by selective laser melting (SLM). Facing the compatibility and cracking problems raised between SiC and metal matrix, great efforts on the suppression of defects during the SLM process are taken from various aspects, including laser melting, substrate preheating, and design of support and build directions. Substrate preheating can be used for the significant suppression of cracks. Tillmann *et al.* treated the IN718 component with the HIP method and the density of components was increased to 99.985%–99.989% within a certain range. However, most of the researches focus on just one kind of defect as well as its corresponding control methods. There are a few summaries of formation mechanisms and control methods of typical defects in LAM of metallic components.

Progress We also summarize and analyze the formation mechanisms and control methods of three types of defects (cracks, inclusions and pores) in LAM of metallic components. The thermal cycle during the LAM process usually causes the generation of large internal stress, which causes the micro-crack formation during or after deposition. According to the formation temperature, cracks can be divided into cold cracks and thermal cracks (Figs. 1 and 2). Pores are always formed due to the insufficient energy input during the deposition process (Fig. 3) or the trapping of the residual gas inside the molten pool, which is related to the flowing behavior of molten metal fluid in the pool (Figs. 4 and 5). There are two main types of inclusion defects: one is oxide inclusions mostly caused by the mixing of oxygen in the production atmosphere, and the other is high-melting metal inclusions caused by the mixing of powders with high-melting metal powders (Fig. 6).

Different control methods are required for different types of alloys and defects. For cold cracks, the currently commonly used control methods include optimizing the compositions of metal powder and adding post-heating treatment. For hot cracks, the currently commonly used control methods include optimizing the compositions of metal powder and the process including selecting appropriate parameters (Fig. 7) and preheating substrates (Fig. 8). The pore defects can be minimized by either improving powder quality (Fig. 9) or adopting post-processing. For high melting-point metallic inclusions, the effective control methods include the selection of reasonable process parameters and scanning schedule. For oxide inclusion defects, the main control method is to control the oxygen content in environment.

Conclusions and Prospects The laser melting deposition additive manufacturing technology for metallic components is a high-performance, low-cost, and designable manufacturing technology. However, the degradation of material properties due to the defects is still one of the problems that must be solved during component production. It is still necessary to conduct a more in-depth research in the following aspects. For crack defects, it is necessary to discuss the stress evolution during the deposition as well as the relationship between mechanical behaviors and internal stress distributions. For pore defects, the quantification of the influence of each process parameter on the formation mechanism is required. For inclusion defects, it needs to research the thermodynamic mechanism of the protective gas composition and their flowing behaviors.

Key words laser technique; materials; laser additive manufacturing; metallic components; defect; control mechanism